CRISPR–Cas9 genome editing induces a p53-mediated DNA damage response

Emma Haapaniemi[1,2,4], Sandeep Botla[1,4], Jenna Persson [ID][1], Bernhard Schmierer[1,5]* and Jussi Taipale[1,2,3,5]*

Here, we report that genome editing by CRISPR–Cas9 induces a p53-mediated DNA damage response and cell cycle arrest in immortalized human retinal pigment epithelial cells, leading to a selection against cells with a functional p53 pathway. Inhibition of p53 prevents the damage response and increases the rate of homologous recombination from a donor template. These results suggest that p53 inhibition may improve the efficiency of genome editing of untransformed cells and that p53 function should be monitored when developing cell-based therapies utilizing CRISPR–Cas9.

Clustered regularly interspaced short palindromic repeats (CRISPR)–CRISPR-associated protein 9 (Cas9) has become a popular precision genome editing tool. DNA double-strand breaks (DSBs) induced by Cas9 are repaired either by the error-prone process of non-homologous end joining (NHEJ) or precisely by pathways using homology-directed repair (HDR). The choice of repair mechanism is dependent on the stage of the cell cycle, with NHEJ predominating in G1 and HDR becoming efficient during DNA replication[1]. The classical HDR mechanism, the DSB repair pathway, is regulated by the cell cycle machinery[1], whereas the cell cycle dependence of other HDR mechanisms, such as synthesis-dependent strand annealing[2], is less well defined. In precision genome editing, a repair template that is homologous to the cut locus is introduced into cells, where it is used by the endogenous HDR machinery to repair the DSB. In an optimal case, these processes lead to a defined and precise editing of the genome.

Precision genome editing by HDR is fairly efficient in some tumor cell lines[3]. By contrast, the genomes of normal cells have been more difficult to edit, because the cells can undergo apoptosis and/or preferentially use NHEJ for damage repair[4,5]. Recently, several promising methods to improve the efficiency of template-dependent genome editing of primary cells have been developed based on increasing the concentration of the repair DNA template, delivering NHEJ inhibitors and optimizing transfection[3,4,6–8]. However, there is no mechanistic explanation for the relative inefficiency of recombination-based editing of normal, untransformed human cells.

During the course of identifying essential genes in a large panel of cell lines using standard CRISPR–Cas9 'dropout' screens[9] (Fig. 1a and Methods), we observed that guide sequences targeting essential genes were not efficiently depleted in retinal pigment epithelium (RPE1) cells. RPE1 cells are non-transformed cells that are immortalized solely by stable human telomerase reverse transcriptase (hTERT) expression. They are derived from human RPE and represent a cell type with substantial medical interest, as malfunctioning RPE is seen in both monogenic and acquired retinal degenerative diseases and is currently a target for retinal regenerative therapies[10].

In RPE1 cells, we noted a dramatic increase in the levels of guides targeting the tumor suppressor *TP53* (encoding p53), its transcriptional target cyclin-dependent kinase inhibitor 1A (*CDKN1A*; encoding p21) and the retinoblastoma gene *RB1* (enconding pRB), which mediates cell cycle arrest downstream of p21 (ref. [11]) (Fig. 1b).

These observations suggest that, in cells with a wild-type p53 response, DSBs induced by Cas9 activate p53, leading to a growth arrest. This explains the selective growth advantage of cells in which the p53–p21–pRB axis is disrupted. The effect also explains the failure to detect essential genes in the CRISPR screen, as all other cutting guide RNAs (gRNA) will cause a transient cell cycle arrest and are thus selected against.

To test this hypothesis, we carried out new genome-wide CRISPR–Cas9 screens in RPE1 cells and in RPE1 cells deficient in p53 (ref. [12]) using a genome-wide library[13]. Consistent with the hypothesis, gene set enrichment analyses on the ranked list of genes[14] identified known essential pathways in $p53^{-/-}$, but not in $p53^{+/+}$ cells (Supplementary Table 1). An example of this phenomenon is shown in Fig. 1c. Guides against ribosomal genes should deplete quickly from the cell pool, as most of their targets are essential for cell viability. In a list ranked by the degree of guide depletion, the gene rank of ribosomal genes is therefore expected to be low. This is indeed the case for RPE1 $p53^{-/-}$ cells (Fig. 1c, left panel), where ribosomal genes concentrate in the lowest decile. By contrast, in RPE1 $p53^{+/+}$ cells, no depletion of guides against ribosomal genes is observed. Non-targeting control guides, which do not have genomic binding sites, behave similarly in $p53^{+/+}$ and $p53^{-/-}$ RPE1 cells, suggesting that the effect is due to on-target DNA cutting and does not result from off-target DSBs.

Conversely, guides targeting p21 were enriched in $p53^{+/+}$ but not in $p53^{-/-}$ cells (4.7-fold versus 0.8-fold, respectively), indicating that loss of p21 only confers a growth advantage in the presence, but not the absence, of p53. We conclude that DSBs introduced by CRISPR–Cas9 trigger a transient, p53-dependent cell cycle arrest mediated through p21 and pRB, irrespective of the locus targeted. This generic penalty of DNA cutting masks guide-specific effects, hampering guide dropout screens that are aimed at identifying genes whose loss leads to cell death or decreased cell proliferation.

In lentiviral screens, Cas9 and the guide sequence are integrated into the genome and are constitutively active. To assess whether the transient Cas9 activity used in precision genome editing approaches would trigger a similar response, we transfected RPE1 $p53^{+/+}$ and $p53^{-/-}$ cells with ribonucleoprotein (RNP) complexes containing Cas9 and a guide. We found that even such a short exposure to Cas9 RNP activity resulted in a partial G1 arrest (Fig. 2a) in $p53^{+/+}$, but not in $p53^{-/-}$, cells. In accordance with the screening results, which

---

[1]Department of Medical Biochemistry and Biophysics, Karolinska Institute, Stockholm, Sweden. [2]Genome-Scale Biology Program, University of Helsinki, Helsinki, Finland. [3]Department of Biochemistry, University of Cambridge, Cambridge, United Kingdom. [4]These authors contributed equally: Emma Haapaniemi, Sandeep Botla. [5]These authors jointly supervised this work: Bernhard Schmierer, Jussi Taipale.
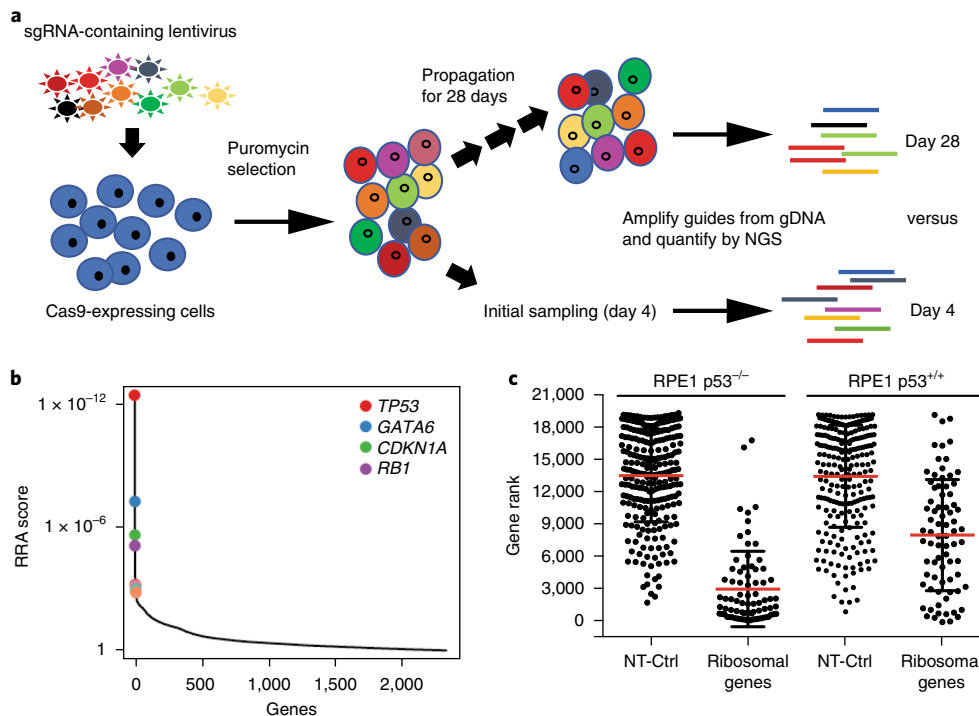*e-mail: bernhard.schmierer@ki.se; ajt208@cam.ac.uk

Fig. 1 | Unbiased CRISPR screening identifies activation of the p53–p21–RB axis. a, Schematic representation of CRISPR screening for fitness genes. Cas9-expressing cells are transduced with pooled lentiviral guide libraries targeting thousands of genes with several guide sequences per gene. Cells are then propagated for several weeks. Guide sequences targeting fitness genes that result in cell death are depleted over time, whereas guides targeting growth inhibitory genes are enriched. Genomic DNA (gDNA) is then prepared from a sample (day 28 after transduction) and a control sample (day 4 after transduction). Guide sequences are amplified by PCR and the relative frequencies of guides in the two populations are determined by next-generation sequencing (NGS). Enrichment or depletion of guide sequences relative to the control are assessed. sgRNA, single-guide RNA. **b**, Modified RRA analysis (with the software package MAGeCK[18]) of genes in immortalized RPE1 p53^{+/+} cells in a screen targeting approximately 2,000 transcription factors and cancer genes. The RRA scores of the top four genes (the genes whose guide sequences were most highly enriched) are highlighted. **c**, The ranking of ribosomal genes in a hit list by the degree of guide sequence depletion in a genome-wide knockout screen in p53^{+/+} and p53^{-/-} RPE1 cells (average rank: 1,627 and 8,034 out of 19,114 genes, respectively; red line). Standard deviations are indicated as error bars. Each of the screens was conducted in two independent replicates; the data shown are representative of one replicate for each screen. NT-Ctrl, non-targeting control guide.

point to p53-dependent cell cycle arrest rather than apoptosis, we did not detect caspase 3 cleavage in response to RNP delivery in RPE1 cells (Supplementary Fig. 1).

Precision genome editing using CRISPR–Cas9 is based on the HDR machinery, which is most active in the S phase[1,11]. Thus, the observed G1 arrest might preclude efficient HDR, instead favoring imprecise repair by NHEJ. This would explain the high NHEJ-mediated insertion and deletion (indel) count and the relatively low efficiency of HDR-dependent precision gene editing in normal cells[4]. p53 inhibition should increase the frequency of HDR and of precision genome editing, as it would permit cell cycle progression in the presence of Cas9-induced DSBs. To test this hypothesis, we used RPE1 p53^{+/+} and p53^{-/-} reporter cell lines expressing a blue fluorescent protein (BFP) and a mutationally inactivated green fluorescent protein (GFP) in which the GFP fluorophore was destroyed by three point mutations (Fig. 2b). Co-transfection with a Cas9 RNP targeting the mutation site of the dead GFP and a single-stranded DNA oligonucleotide template restores GFP fluorescence, if repair occurs by template-dependent gene correction.

As expected, primary and immortalized RPE1 p53^{+/+} cells showed less efficient gene correction than p53^{-/-} cells (Fig. 2c). The CDK4/6 inhibitor palbociclib, which arrests cells in G1, decreased GFP repair by 50% in both cell lines, providing further evidence that stalled cell cycle progression hampers precision genome editing (Fig. 2d and Supplementary Fig. 2). Co-transfection of the p53 antagonist MDM2 dose dependently improved the repair efficiency

in the p53^{+/+} line (Fig. 2e). This effect was inhibited by nutlin-3a (Fig. 2f), a compound that specifically abolishes the p53–MDM2 interaction, indicating that improved repair in response to MDM2 overexpression is mainly due to MDM2-dependent p53 degradation. However, MDM2 loss may also have p53-independent effects that stimulate gene correction. Taken together, these data indicate that p53 activation causes a G1 arrest, which in turn decreases the efficiency of precision genome editing from a repair template. However, we cannot rule out that other mechanisms act downstream or parallel to p53 in limiting the efficiency of precision genome editing in normal human cells[15,16].

Growth arrest and apoptosis upon delivery of Cas9 RNP complexes into cells have been attributed to a type I interferon (IFN) response, which can be activated by plasmid or protein transfection, as well as lentiviral transduction[6,17]. However, inhibitors of the IFN-α, interleukin-1β and Toll-like receptor signaling—the pathways comprising the main arms of the pathogen-sensing machinery—failed to improve the efficiency of genome editing in p53^{+/+} RPE1 cells (Supplementary Table 2). These results suggest that the type I IFN response alone does not explain the observed CRISPR–Cas9 toxicity and G1 arrest in RPE1 cells.

We report here that genome editing by Cas9 in p53-proficient cells results in a DNA damage response, which causes a growth disadvantage/arrest, and decreases efficiency of precision genome editing. The observed effect is dependent on p53, its direct target p21 and on pRB, which mediates the G1 cell cycle arrest in response
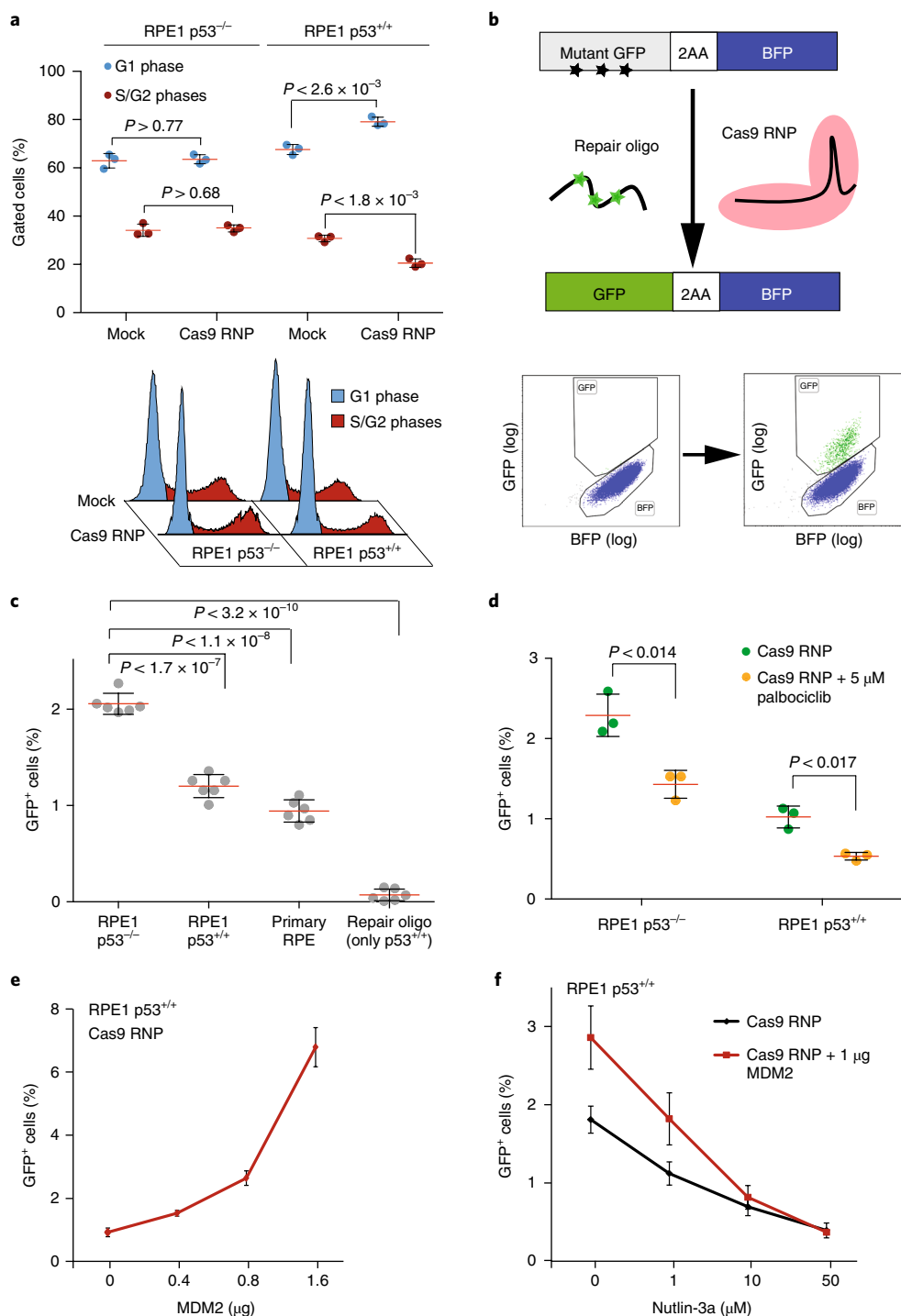
Fig. 2 | Cas9 gRNA RNP delivery triggers a p53-dependent DNA damage response that suppresses gene correction. a, Top panel: the cell cycle status in p53^{+/+} and p53^{−/−} RPE1 cells transfected with Cas9 RNP ($n = 3$ biologically independent samples, representative replicate of two independent experiments). Bottom panel: representative cell cycle histograms from RPE1 cells ($n = 1$) transfected with Cas9 RNP. Mock, transfection reagent only. **b**, Top panel: schematic representation of the BFP–GFP reporter system. The efficiency of gene correction is evaluated by the percentage of cells that turn GFP-positive upon cutting and precision repair by a donor template. Bottom panel: FACS plots illustrating GFP reporter detection in RPE1 cells (left, before editing; right, after successful GFP repair; representative of one replicate in Fig. 2c). **c**, GFP editing efficiency in p53^{+/+} and p53^{−/−} RPE1 cells and in primary RPE cells, as well as after transfection of the repair oligo without Cas9 RNP in p53^{+/+} RPE1 cells ($n = 6$ biologically independent samples, representative replicate of two independent experiments). **d**, GFP editing efficiency in p53^{+/+} and p53^{−/−} RPE1 cells treated without or with the CDK4/6 inhibitor palbociclib ($n = 3$ biologically independent samples, representative replicate of two independent experiments). **e**, GFP editing efficiency in p53^{+/+} RPE1 cells transfected with increasing amounts of MDM2 plasmid ($n = 6$ biologically independent samples, representative replicate of two independent experiments). **f**, GFP editing efficiency in p53^{+/+} RPE1 cells with or with MDM2 plasmid transfection and treated with increasing concentrations of nutlin-3a, an antagonist of the p53–MDM2 interaction ($n = 6$ biologically independent samples). All data sets were acquired by flow cytometry, and significance was calculated using a two-tailed Welch's t-test. The red line represents the mean; the error bars represent standard deviations. For representative dot-blots and/or histograms indicating the gating, see Supplementary Figs. 3–5.

to p21 (ref. [11]). The effect depends on the presence of DNA DSBs, as cells harboring non-targeting gRNAs are enriched in the RPE1 essentiality screen, indicating that non-cutting gRNAs do not induce a growth arrest (Fig. 1c). The general effect of all gRNAs irrespective of their genomic targets, in turn, suggests that very few DSBs are sufficient for the growth arrest. Cas9 has been shown to remain associated with cut sites for over 6 hours after the DSB[3], perhaps preventing a successful repair and/or causing stalled replication forks, which might amplify the effect of a single DSB.

Our results show that inhibiting DNA damage signaling can improve the efficiency of precision genome editing in normal, untransformed cells. However, inhibition of p53 leaves the cell transiently vulnerable to the introduction of chromosomal rearrangements and other tumorigenic mutations. Temporary inhibition of p53 in normal cells will have both positive and negative effects on the tumorigenic potential of the edited cell population. On the one hand, it could potentially allow the escape of cells whose genome is damaged during the editing process itself. On the other hand, it will increase the editing efficiency and decrease the selective advantage of pre-existing p53-deficient clones. To improve the balance, future work should focus on understanding the DNA damage response induced by Cas9. Controlling DNA damage signaling, such that efficient gene correction can occur but the formation and selection of potentially tumorigenic cells are suppressed, will be important in developing safer and more efficient next-generation genome editing technologies.

Methods

Methods, including statements of data availability and any associated accession codes and references, are available at https://doi.org/10.1038/s41591-018-0049-z.

References

1. Hustedt, N. & Durocher, D. *Nat. Cell Biol.* **19**, 1–9 (2016).
2. Hohmann, S. & Gozalbo, D. *Mol. Gen. Genet.* **211**, 446–454 (1988).
3. Richardson, C. D., Ray, G. J., DeWitt, M. A., Curie, G. L. & Corn, J. E. *Nat. Biotechnol.* **34**, 339–344 (2016).
4. DeWitt, M. A. et al. *Sci. Transl. Med.* **8**, 360ra134 (2016).
5. Yin, H. et al. *Nat. Biotechnol.* **32**, 551–553 (2014).
6. Dever, D. P. et al. *Nature* **539**, 384–389 (2016).
7. Lee, K. et al. *eLife* **6**, e25312 (2017).
8. Maruyama, T. et al. *Nat. Biotechnol.* **33**, 538–542 (2015).
9. Schmierer, B. et al. *Mol. Syst. Biol.* **13**, 945 (2017).
10. Luo, M. & Chen, Y. *Int. J. Ophthalmol.* **11**, 150–159 (2018).
11. Otto, T. & Sicinski, P. *Nat. Rev. Cancer* **17**, 93–115 (2017).
12. Sokolova, M. et al. *Cell Cycle* **16**, 189–199 (2017).
13. Doench, J. G. et al. *Nat. Biotechnol.* **34**, 184–191 (2016).
14. Wang, J., Vasaikar, S., Shi, Z., Greer, M. & Zhang, B. *Nucleic Acids Res.* **45**, W130–W137 (2017).
15. Canny, M. D. et al. *Nat. Biotechnol.* **36**, 95–102 (2018).
16. Cuella-Martin, R. et al. *Mol. Cell* **64**, 51–64 (2016).
17. Muerdter, F. et al. *Nat. Methods* **15**, 141–149 (2018).
18. Li, W. et al. *Genome Biol.* **15**, 554 (2014).

Acknowledgements

Author contributions

E.H., B.S. and J.T. wrote the manuscript. S.B., B.S. and J.P. conducted the genome-wide knockout screens. E.H., B.S. and S.B. prepared the cell lines and performed the flow cytometry experiments. J.T. and B.S. supervised the study. All authors read and approved the final manuscript.

Competing interests

The authors declare no competing interests.

Additional information

Methods

Genome-wide essentiality screen with the transcribed random sequence library strategy. This method was used in the initial screening of 15 tumor cell lines (data not shown) and detected p53 pathway targeting in RPE1 p53^{+/+} cells[9]. The screen was performed in duplicate.

Oligo synthesis and library cloning. Oligo pools were ordered from CustomArray. The guide sequences for all libraries used are given in the Supplementary File, GuideSequences.xlsx. The oligos were designed to contain six random bases (B6) and a 20-nucleotide guide sequence (N20). All guide sequences were taken from previously published, genome-wide libraries[19].

Oligo sequence:
5′-GCTTTATATATCTTGTGGAAAGGACGAAACACCG-B6-N20-GTTTTA GAGCTAGAAATAGCAAGTTAAAATAAGGCTAGTCCG-3′

Oligo double stranding was done by PCR using the primers:
Ds-fw: 5′-GTATTTCGATTTCTTGGCTTTATATATCTTGTGGAAAGGACG-3′
Ds-rev: 5′-CGGACTAGCCTTATTTTAACTTGC-3′

The double-stranded PCR product was gel purified and cloned into the lentiviral vector pLenti-Guide Puro (Addgene 52963) by Gibson assembly. The assembly reaction was diluted 1:10 in water and transformed into electrocompetent *Escherichia coli* (E. cloni 10 G SUPREME, Lucigen). A total of ~4,000,000 colonies were obtained, corresponding to an average of ~300 colonies (and therefore ~300 random sequence libraries) per each of the 12,472 guide sets.

Library packaging. The library was packaged in HEK293T cells by transfecting with the library plasmid and the two packaging plasmids psPAX2 (Addgene 12260) and pCMV-VSV-G (Addgene 8454) in equimolar ratios. After 48 h, the virus-containing supernatant was concentrated 40-fold using Lenti-X concentrator (Clontech), and single-use aliquots were prepared and stored at −140 °C.

Creating editing-proficient Cas9 cell lines. Cells were transduced with a lentivirus containing the plasmid pLenti-Cas9-Blast-sgHPRT, which contains both wild-type Cas9 and a guide sequence against the *HPRT1* gene (GATGTGATGAAGGAGATGGG). Forty-eight hours after transduction, cells were selected with 5 μg ml⁻¹ blasticidin for Cas9 expression for 7–10 days, and afterwards with 5 μg ml⁻¹ 6-thioguanine for 7–14 days to select editing-proficient cells in which *HPRT1* had been disrupted.

Library transduction. A minimum of 100 million RPE1 Cas9 cells were transduced with the library virus at a multiplicity of infection of 0.5. Cells were then selected for guide integration with 1 μg ml⁻¹ puromycin for 4 days.

Cell propagation and sample preparation. Cells were kept in culture for a total of 28 days after transduction by subculturing them every 3–4 days, always keeping cell numbers close to 100 million. Genomic DNA was prepared from 40 million cells (~200 μg genomic DNA) at day 4 and day 28 after transduction. Day 4 after transduction was used as the control time point.

Preparation of the sequencing library from genomic DNA. Approximately 200 μg genomic DNA in 40 parallel reactions were used. Fourteen cycles were run and the reactions were pooled together. PCR1 amplifies the genomic region containing the guide sequence. PCR2 and PCR3 then incorporate the Illumina sequencing adaptors with primers 2F/2R and 3F/3R, respectively. 3R contains the Illumina index for multiplexing, indicate by NNNNNN in the sequence given.

1FGGACTATCATATGCTTACCGTAACTTGAAAGTATTTCG
1RCTTTTAGTTTGTATGTCTGTTGCTATTATGTCTACTATTCTTTCC
2FACACTCTTTCCCTACACGACGCTCTTCCGATCTCT-TGTGGAAAGGACGAAACAC
2RAGACGTGTGCTCTTCCGATCTCTACTATTCTTTCCCCTGCACTGT-3′
3FAATGATACGGCGACCACCGAGATCTACACTC-TTTCCCTACACGACGC
3RCAAGCAGAAGACGGCATACGAGAT(N6) GTGACTGGAGTTCAGACGTGTGCTCTTCCGATCTCTAC

Sequencing was done with the custom sequencing primer CRISPR_Seq and the standard Illumina index read primer:
CRISPR_SeqCGATCTCTTGTGGAAAGGACGAAACACCG
Index read primerGATCGGAAGAGCACACGTCTGAACTCCAGTCAC

PCR2 used 5 μl of pooled PCR1 as template and was run for 18 cycles. PCR3 used 2 μl of PCR2 as template and was run for 14 cycles. The resulting product of 350 bp was gel purified and sequenced on an Illumina HiSeq 2000 instrument, multiplexing 4–6 samples per lane.

Genome-wide essentiality screen with the Brunello library. This screening method was used to verify the initial result of the p53 pathway knockdown seen in RPE1 cells after transcribed random sequence library screening[13]. We used p53^{+/+} and p53^{−/−} RPE1 cells. A single replicate was used for both cell lines.

Library packaging. The Brunello guide library (Addgene 73178), which targets 19,114 human genes with 4 guides each[13] was packaged in HEK293T cells as described above.

Generation of the Cas9 cell line. Editing-proficient, Cas9-expressing, p53-deficient hTERT-RPE1 cells[12] were generated as described above.

Genome-wide screen and sequencing library preparation. Populations of 80 million cells each of hTERT-RPE1 p53^{+/+} (ATCC CRL-4000) and hTERT-RPE1 p53^{−/−} were transduced with the Brunello guide library. Cells were then propagated for 28 days, with subculture every 3–4 days and 80 million cells were reseeded after each split. Samples of 75 million cells were harvested on post-transduction day 4 and day 28, from which genomic DNA was isolated using Qiagen Blood and Tissue Maxi columns. Guide sequences were then amplified from 150 μg genomic DNA in 30 parallel reactions with primers and cycles as described above. The final PCR product was gel purified using Freeze 'N Squeeze columns (Bio-Rad) and sequenced on an Illumina HiSeq 2500 instrument.

Data analysis. The data analysis was performed using the MAGeCK pipeline[18]. Briefly, MAGeCK aligns the sequencing reads to the gRNA library file to obtain the read count per guide. These read counts are then normalized, and P values or false discovery rates are calculated for enrichment and depletion of each guide at day 28 compared to day 4. The consistency of the behavior of all guides targeting the same gene is then used to calculate the robust rank aggregation (RRA) score, to call both positively and negatively selected genes.

Cell culture and GFP reporter cell line. hTERT immortalized RPE1 cells were obtained from the American Type Culture Collection (ATCC) and cultured at 37 °C in a humidified incubator in DMEM supplemented with 10% FCS, 1% glutamine and 1% penicillin–streptomycin. Primary RPE1 cells were obtained from Lonza and were cultured in RPE Cell Basal Medium (RtEGM, Lonza) supplemented with 2% FBS and growth factors according to the manufacturer's recommendation.

For easy detection of homologous recombination triggered by CRISPR–Cas9, we created a cassette encoding a Zeocin resistance gene for selecting stable integrants, a mutant GFP (37 amino acid (AA)-38AA-39AA) sequence and a BFP sequence separated from GFP by a 2AA self-cleaving plasmid. This cassette was transduced to p53^{−/−}, p53^{+/+} and primary RPE1 cells by lentivirus; the lentiviral packaging is described above. Based on the assessment of constitutive BFP expression, the copy number distribution of the cassette is similar in p53^{−/−} and p53^{+/+} cells (see Supplementary Fig. 5). When Cas9 along with a repair template correcting the GFP mutation is introduced into these cell lines, gene correction will give rise to functional GFP. GFP fluorescence was measured by fluorescence-activated cell sorting (FACS) after 4 days, if Cas9 was delivered as a plasmid, or 3 days, if Cas9 was delivered as an RNP.

GFP CRISPR RNA sequence:
CTGCCAAGCTGACCCTGAAG
GFP repair oligo template sequence:
GAACGGCCACAAGTTCAGCGTGTCCGGCGAGGGCGAAGGCGACGC CACATATGGCAAGCTGACCCTGAAGTTCATCTGCACCACCGGCAAGCTG CCCGTG

RNP transfection. We obtained the CRISPR RNAs (crRNAs) and the trans-activating crRNAs (tracrRNAs) from Integrated DNA Technologies and wild-type *Streptococcus pyogenes* spCas9 from Integrated DNA Technologies, Eupheria Biotech or custom produced at the Protein Science Facility at the Karolinska Institute. The different protein sources might be responsible for some of the experimental variability seen in Fig. 2c–f.

crRNA/tracrRNA hybridization and RNP complex formation were done according to the manufacturer's instructions. For transfection, cells were plated in 48-well plates (for the GFP reporter assay) or 10-cm plates (for the cell cycle assay) and transfected with 13 pmol (48-well plates) or 400 pmol (10-cm plates) of RNP and 10 pmol of repair DNA template (48-well plates) using the CRISPRmax transfection reagent (Thermo Scientific) according to the manufacturer's instructions.

For cleaved caspase 3 and cell cycle analysis, we used an RNF2 locus guide, which seems to have no off-target effects[20] (crRNA sequence: GTCATCTTAGTCATTACCTG).

FACS. For the detection of corrected GFP, the RNP-transfected cells were cultured for 3 days, as described in the 'Genome-wide essentiality screen with the Brunello library' section, trypsinized, resuspended in warm culture medium and immediately subjected to FACS (Supplementary Figs. 3–5).

For cleaved caspase 3 antibody staining (Alexa-488 conjugate, 9669S, Cell Signaling), the cells were transfected with RNPs, incubated for 48 h, trypsinized, permeabilized by 0.05% Triton X-100 and fixed using 1% paraformaldehyde. We used PBS supplemented with 10% FCS and 3% BSA for blocking, and incubated cells overnight with the primary antibody at 1:100 dilution in a final volume of 300 μl. The next day, cells were washed twice and subjected to FACS. The cell cycle stage was analyzed by FxCycle Violet stain (Invitrogen). All data were acquired using a Cyan II flow cytometer (Beckman Coulter), which is optimized for high-throughput readout. The data were analyzed using Kaluza v.1.2. (Beckman Coulter). Linear detection was used for FxCycle and cleaved caspase 3, and logarithmic detection was used for GFP. All assays were run in triplicates and

replicated three times (one representative replicate is shown in Fig. 2). Welch's *t*-test was used to evaluate statistical significance.

In the palbociclib-treated samples, the cell cycle stage was determined using propidium iodide staining. Briefly, the cells were trypsinized, fixed with 2% paraformaldehyde for 10 min and permeabilized using 0.05% Triton X-100 for 1 h. After washing, the cells were incubated in 37 °C in PBS containing 200 μg ml^{-1} RNAse and 1 mg ml^{-1} propidium iodide in PBS for 1 h. The cells were flow-sorted immediately.

Inhibition of the p53-dependent DNA damage response and type I IFN signaling. MDM2 was purchased from Abcam (ab82080; Fig. 2e) or custom made by GenScript (GST-fusion; Fig. 2f). The different protein sources might be responsible for some of the experimental variability seen in Fig. 2e,f. The proteins were co-transfected in the indicated amounts, with CRISPR–Cas9 RNPs targeting mutant GFP, as described in the 'Cell culture and GFP reporter cell line' section. If applicable, cells were treated with nutlin-3a or palbociclib (Sigma-Aldrich) in indicated amounts at the time of transfection. All assays were run in six parallel wells. Welch's *t*-test was used to evaluate statistical significance.

We used various compounds to inhibit type I IFN signaling; they were added into the cell culture 1–6 h prior to RNP transfection. Their effect on homologous recombination was evaluated as described in the 'Genome-wide essentiality screen with the Brunello library' section. Supplementary Table 2 lists all the tested compounds. All assays were run in triplicates. Welch's *t*-test was used to evaluate statistical significance.

Statistics. *High-throughput screening.* This article describes two different high-throughput screens:

- A screen with 23,279 guides targeting transcription factor and cancer genes[9]. This screen was done in RPE1 p53$^{+/+}$ cells in two independent biological duplicates, with cell culture, sample preparation and next-generation sequencing occurring in different time points between the replicates.
- A genome-wide knockout screen with 77,441 guides[13]. This screen was done in both RPE1 p53+/+ and RPE1 p53−/− cells. Both cell lines were processed in two independent biological replicates.

Validation experiments. To test the statistical significance of the results shown in Fig. 2 as well as in Supplementary Figs. 1 and 2, we used a two-tailed Welch's *t*-test. The statistical parameters for these experiments are shown in the Methods and in Supplementary Table 3. All experiments were performed at least twice, and one representative experiment is shown in all panels.

- Figure 2a and Supplementary Fig. 1: three replicates (=parallel wells in a cell culture plate) for each condition ($n = 3$).
- Figure 2c: six replicates (=parallel wells in a cell culture plate) for each cell type ($n = 6$).
- Figure 2d: three replicates (=parallel wells in a cell culture plate) for each condition ($n = 3$).
- Figure 2e: six replicates (=parallel wells in a cell culture plate) for each condition ($n = 6$).
- Figure 2f: six replicates (=parallel wells in a cell culture plate) for each condition ($n = 6$).
- Supplementary Fig. 2: three replicates (=parallel wells in a cell culture plate) for each condition ($n = 3$).

Reporting Summary. Further information on experimental design is available in the Nature Research Reporting Summary linked to this article.

Code availability. No custom code was used.

Data availability. The raw data can be obtained from corresponding authors upon request.

References
19. Wang, T. et al. *Science* **350**, 1096–1101 (2015).
20. Tsai, S. Q. et al. *Nat. Biotechnol.* **33**, 187–197 (2015).

nature research

Corresponding author(s):   Jussi Taipale, Bernhard Schmierer

☐ Initial submission   ☐ Revised version   ☒ Final submission

Life Sciences Reporting Summary

Nature Research wishes to improve the reproducibility of the work that we publish. This form is intended for publication with all accepted life science papers and provides structure for consistency and transparency in reporting. Every life science submission will use this form; some list items might not apply to an individual manuscript, but all fields must be completed for clarity.

For further information on the points included in this form, see Reporting Life Sciences Research. For further information on Nature Research policies, including our data availability policy, see Authors & Referees and the Editorial Policy Checklist.

▶ Experimental design

1. **Sample size**

   Describe how sample size was determined.

   No a prior sample size determination was done however all experiments were reproduced and performed in a sufficient number of replicates to determine differences with clear statistical significance.

2. **Data exclusions**

   Describe any data exclusions.

   No exclusions

3. **Replication**

   Describe whether the experimental findings were reliably reproduced.

   For flow cytometry, the samples were run in triplicates or quadruplicates and repeated once (n=2x3 or n=2x4), yielding consistent results. Both CRISPR screens were performed in duplicate, yielding consistent results between replicates and between screens.

4. **Randomization**

   Describe how samples/organisms/participants were allocated into experimental groups.

   For the high-throughput screens, cells were infected with a pool of sgRNA-containing lentiviruses. The same pool of infected cells was propagated in culture flasks and used to derive case (harvested at day 28) and control (harvested at day 4) samples. To obtain a duplicate experiment, the process was repeated for a new batch of cells.

   For flow cytometry validation experiments, cells were grown in culture flasks and split to wells in 48- or 6-well plates, with experimental treatments in separate wells. One plate was treated as a single biological replicate.

   For independent experimental replicates, a new batch of cells was split to new plates, and a new set of reagents were prepared.

5. **Blinding**

   Describe whether the investigators were blinded to group allocation during data collection and/or analysis.

   High-throughput genome-wide or Transcription factor CRISPR/Cas9 screens were unbiased loss of function assays, where hits were called based on rigorous statistical analysis. Theerefore, it is not necessary to blind the experiment.

   The flow cytometry data was acquired by HyperCyte high throughput readout system, which acquires data from each well of a plate at defined speed and time. The data was analyzed as batch analysis, with same gates applied to all samples in a condition. Such automated and computational analysis of data eliminates most of human error and assumption, and we thus we did not blind the final results from the investigators.

Note: all studies involving animals and/or human research participants must disclose whether blinding and randomization were used.

6. Statistical parameters

For all figures and tables that use statistical methods, confirm that the following items are present in relevant figure legends (or in the Methods section if additional space is needed).

n/a	Confirmed	
☐	☒	The <u>exact sample size</u> (*n*) for each experimental group/condition, given as a discrete number and unit of measurement (animals, litters, cultures, etc.)
☐	☒	A description of how samples were collected, noting whether measurements were taken from distinct samples or whether the same sample was measured repeatedly
☐	☒	A statement indicating how many times each experiment was replicated
☐	☒	The statistical test(s) used and whether they are one- or two-sided (note: only common tests should be described solely by name; more complex techniques should be described in the Methods section)
☒	☐	A description of any assumptions or corrections, such as an adjustment for multiple comparisons
☐	☒	The test results (e.g. *P* values) given as exact values whenever possible and with confidence intervals noted
☐	☒	A clear description of statistics including <u>central tendency</u> (e.g. median, mean) and <u>variation</u> (e.g. standard deviation, interquartile range)
☐	☒	Clearly defined error bars

See the web collection on statistics for biologists for further resources and guidance.

▶ Software

Policy information about availability of computer code

7. Software

Describe the software used to analyze the data in this study.	MAGeCK (version 0.5.6) Excel 2013, Kaluza (version 1.2), R (custom code used to separate individual wells from 48-well plate flow cytometry readout. The code is available from the corresponding authors upon request.)

For manuscripts utilizing custom algorithms or software that are central to the paper but not yet described in the published literature, software must be made available to editors and reviewers upon request. We strongly encourage code deposition in a community repository (e.g. GitHub). *Nature Methods* guidance for providing algorithms and software for publication provides further information on this topic.

▶ Materials and reagents

Policy information about availability of materials

8. Materials availability

Indicate whether there are restrictions on availability of unique materials or if these materials are only available for distribution by a for-profit company.	No restrictions

9. Antibodies

| Describe the antibodies used and how they were validated for use in the system under study (i.e. assay and species). | cleaved caspase 3: cat no # 9669S, Alexa-488 conjugate, Cell Signaling, clone D175, lot 27. 1:100 dilution in 1% bovine serum albumin+10% fetal calf serum in phosphate-buffered saline.

The antibody was validated by staining cisplatin-treated RPE-1 cells and detecting upregulation of caspase 3 in these cells (data not shown). The production company has also validated the antibodies for cells and tissues of human origin, and demonstrated that the antibody detects upregulation of CC3 in ICC and flow cytometry applications. |
|---|---|

10. Eukaryotic cell lines

a. State the source of each eukaryotic cell line used.

hTert immortalized Retinal Pigment Epithelium cells were purchased from ATCC, and primary Retinal Pigment Epithelium cells from Lonza. HEK293T cells (to prepare lentiviral constructs for crispr screens) were purchased from ATCC.

b. Describe the method of cell line authentication used.

Cell lines were purchased directly from the vendor. Both Lonza and ATCC use short tandem repeat (STR) profiling to confirm identity of the cell lines. In addition, the cell morphology was consistent with RPE-1 and HEK293T cell morphology.

c. Report whether the cell lines were tested for mycoplasma contamination.

All cell lines tested negative for mycoplasma during the time of the study. We used the MycoAlert™ kit from Lonza, cat no # LT07-418 for mycoplasma detection.

d. If any of the cell lines used are listed in the database of commonly misidentified cell lines maintained by ICLAC, provide a scientific rationale for their use.

No misidentified cell lines were used in the study.

▸ Animals and human research participants

Policy information about studies involving animals; when reporting animal research, follow the ARRIVE guidelines

11. Description of research animals

Provide details on animals and/or animal-derived materials used in the study.

No animals were used in the study.

Policy information about studies involving human research participants

12. Description of human research participants

Describe the covariate-relevant population characteristics of the human research participants.

No human participants were used in the study.

nature research

Corresponding author(s):   Jussi Taipale, Bernhard Schmierer

☐ Initial submission   ☐ Revised version   ☒ Final submission

Flow Cytometry Reporting Summary

Form fields will expand as needed. Please do not leave fields blank.

▶ Data presentation

For all flow cytometry data, confirm that:

☒ 1. The axis labels state the marker and fluorochrome used (e.g. CD4-FITC).

☒ 2. The axis scales are clearly visible. Include numbers along axes only for bottom left plot of group (a 'group' is an analysis of identical markers).

☒ 3. All plots are contour plots with outliers or pseudocolor plots.

☒ 4. A numerical value for number of cells or percentage (with statistics) is provided.

▶ Methodological details

5.	Describe the sample preparation.	For GFP detection, RNP-transfected cells were cultured for 3 days, trypsinized, resuspended in warm culture medium and immediately subjected to FACS. For cell cycle analysis and cleaved caspase 3 (cat no # 9669S, Alexa-488 conjugate, Cell Signaling) stainings, the cells were transfected with RNPs, incubated for 24h, trypsinized, permeabilized by 0.05% Triton-X and fixed using 1% paraformaldehyde. Blocking was done in PBS/10% FCS/3% BSA, antibody incubation overnight at 1:100 dilution. Cells were washed twice in PBS and subjected to FACS. Cell cycle phase was determined using FxCycle Violet stain (Invitrogen), according to manufacturer's instructions. Linear detection was used for FxCycle and cleaved caspase 3, and logarithmic detection for GFP.
6.	Identify the instrument used for data collection.	Cyan II Flow Cytometer (Beckman Coulter)
7.	Describe the software used to collect and analyze the flow cytometry data.	Kaluza Flow Cytometry Analysis v1.2
8.	Describe the abundance of the relevant cell populations within post-sort fractions.	>10 000 cells per fraction
9.	Describe the gating strategy used.	The cell population was defined by plotting SS against FS, doublets were excluded by plotting pulswidth against FS. Linear detection was used for cleaved caspase 3, and logarithmic detection for GFP.

Tick this box to confirm that a figure exemplifying the gating strategy is provided in the Supplementary Information. ☒